Vacancies and holes in bulk and at 180° domain walls in lead titanate

Charles Paillard, Grégory Geneste, Laurent Bellaiche, Brahim Dkhil

Vacancies and holes in bulk and at 180° Domain Walls in Lead Titanate

Charles Paillard[1,2]*, Grégory Geneste[3]*, Laurent Bellaiche[2] and Brahim Dkhil[1]

[1]Laboratoire SPMS, CentraleSupélec/CNRS UMR8580, Université Paris-Saclay, F-91192 Gif-sur-Yvette, France
[2]Physics Department and Institute for Nanoscience and Engineering, University of Arkansas, Fayetteville, Arkansas, 72701, USA
[3]CEA, DAM, DIF, F-91297 Arpajon, France
[4]Physics Department and Institute for Nanoscience and Engineering, University of Arkansas, Fayetteville, Arkansas, 72701, USA
E-mail: paillard@uark.edu, gregory.geneste@cea.fr

Keywords: ferroelectrics, domain walls

Domain Walls (DWs) in ferroic materials exhibit a plethora of unexpected properties that are different from the adjacent ferroic domains. Still, the intrinsic/extrinsic origin of these properties remains an open question. Here, density functional theory calculations are used to investigate the interaction between vacancies and 180° DWs in the prototypical ferroelectric $PbTiO_3$, with a special emphasis on cationic vacancies and released holes. All vacancies are more easily formed within the DW than in the domains. This is interpreted, using a phenomenological model, as the partial compensation of an extra-tensile stress when the defect is created inside the DW. Oxygen vacancies are found to be always fully ionized, independently of the thermodynamic conditions, while cationic vacancies can be either neutral or partially ionized (oxygen-rich conditions), or fully ionized (oxygen-poor conditions). Therefore, in oxidizing conditions, holes are induced by neutral and partially ionized Pb vacancies. In the bulk $PbTiO_3$, these holes are more stable as delocalized rather than small polarons, but at DWs, the two forms are found to be possible.

1. Introduction

Domain walls (DWs) are interfaces that form in ferroelectric materials due to the competition of the depolarizing field with the elastic energy. They exhibit potentially enhanced or even new properties at the nanoscale, such as higher electrical conductivity than the bulk in $BiFeO_3$[1-3] and $(Pb,La)(Zr,Ti)O_3$ [4], superconductivity in WO_3 [5], polar activity in $CaTiO_3$ and $SrTiO_3$ [6,7], or may even serve as nanoscale chemical reactor in $TbMnO_3$ [8]. Phase transitions restricted to the DW have also been suggested [9-10]. Nowadays, the possibility of probing the nanoscale has made the interest in DWs soar [11-12] and the control of their nucleation, motion and positioning opens the door towards applications [13-14]. However, the question remains on how much of these new/enhanced properties is intrinsic to the DW, and how much originates from extrinsic causes, for instance single point defects. Indeed, the latter, such as oxygen vacancies, have shown a natural tendency to pin DWs [15-17], cause fatigue and imprint [18-19], and easily form complexes with metal impurities [17,20], forming local dipoles.

Defects are also natural sources of free charges that can be released [21-22], or captured, and which may couple strongly enough to the lattice in ionic polar systems to form polarons [23]. The charges potentially released can accumulate at the DW, possibly explaining the observed enhanced conductivity of DWs [1,2,4], and can also stabilize head-to-head or tail-to-tail charged DWs. Therefore, a deep understanding of the formation of defects at DWs is much needed, in order to reveal the implication of defects in the peculiar properties of DWs, and provide an alternative route to manipulate the DWs functionalities through what we may call "defectronics".

The present work is focused on vacancies in lead titanate, a prototypical ferroelectric, the simplest system to start with in order to have a clear understanding of the mechanisms ruling

the formation of single point defects, their interaction with DWs and the nature of the free charges they may release.

2. Methods

2.1. Density-functional calculations

Density-Functional Theory (DFT) allows to achieve a fundamental understanding of the formation of defects in oxides. We therefore studied a 6x2x2 supercell of lead titanate (120 atoms), shown in Fig. (1), containing two 180° PbO-centered DWs, and in which the defects (vacancies) are introduced in different sites and different charge states. O_3 denotes the apical oxygen, while O_1 and O_2 are the equatorial ones. We used the ABINIT code [24], with the Local Spin Density Approximation (LSDA) exchange-correlation functional [25-26], and also the LSDA$+U$ functional (see below), with the Projector Augmented Wave (PAW) [27-28] method. The LSDA was chosen because it correctly describes the ferroelectric (FE) distortion and tetragonality in PTO, while GGA provides poor description of tetragonal FE PTO (it strongly overestimates the tetragonality). A plane wave cut-off of 20 Ha is employed, corresponding to a convergence of the energy difference between the five-atom ferroelectric *P4mm* and paraelectric *Pm-3m* structures smaller than 1 meV. The PAW double grid cut-off energy value is 30 Ha and a 6x6x6 (resp. 1x3x3) *k*-point mesh was used for the 5-atom cell (resp. 120-atom supercell). The calculated in-plane lattice constant of the tetragonal cell is 3.871 Å, the *c/a* ratio is 1.046, and our computed value of the formation energy of the PbO (resp. TiO_2)-centered 180° domain wall (125.5 and 168.2 $mJ.m^{-2}$ respectively), are all in very good agreement with earlier works [29-31], confirming, in particular, that the PbO-centered 180° DW (simulated here) is more stable than the TiO_2-centered one. The atomic displacements of the 5-atom $PbTiO_3$ ferroelectric unit cell are mostly recovered at the center

of the domains (a region referred to bulk), consistent with a two unit cells wide DW (see Table S1 in the Supplementary Information) [29].

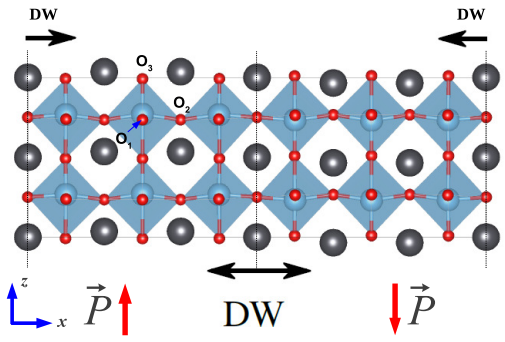

Figure 1. View of the supercell used in the present calculations.

Formation Energy of defects

The formation energy of a defect D in charge state q, can be computed from DFT according to the following expression [32-34]

$$\Delta E^{0}_{D,q} = \left[E_{KS,D,q} - E_{KS,H}\right] + q(E_v + \mu_F) + \sum_i \mu_i dn_i \qquad (1)$$

with $E_{KS,D,q}$ being the total energy of the supercell with the defect D in charge state q, $E_{KS,H}$ that of the pristine supercell, E_v is the top of the valence band, and μ_F the Fermi level ($0 \leq \mu_F \leq E_g$, E_g being the band-gap). μ_i is the chemical potential of species i, and dn_i is the change of the number of atoms of species i associated with the creation of defect D.

Periodic DFT calculations of point defects need *a posteriori* corrections, and we mostly refer to the correction scheme detailed in Refs. [32,34] Because of the periodic boundary conditions (PBCs), the electrostatic interaction of defects with their replica is corrected using the monopole term of the Makov-Payne correction [35-36]. The PBCs also cause an artificial periodicity of the defects, thereby creating a defect band rather than a single state. This so-called band-filling effect [32,34] was corrected as well. Moreover, the calculation of charged defects in a periodic supercell introduces a shift of the electrostatic potential, which is aligned [32,34] using the deep *3s* semicore states of the titanium atoms

[21]. Eventually, one of the major problems of the LSDA functional is the underestimation of the band gap. The calculated band gap within the LSDA is 1.52 eV, while the true band gap lies around 3.4 eV [18,37]. To correct for this anomaly, it is necessary to shift the top of the valence band (or Valence Band Maximum) (VBM) and the bottom of the conduction band (or Conduction Band Minimum) (CBM) in order to recover the true bandgap, and shift shallow levels accordingly, while leaving deep states untouched [32]. Those shifts must then be included in Eq. (1). Since the eigenvalue of the highest occupied level (valence band top E_v) is related to the ionization potential [38-39] in finite system, we performed a surface calculation [39-40] to determine the shift of the valence band, -0.53 eV (by comparison with the experimental ionization potential, -6.2 eV [37]). The CBM was then shifted in order to recover the experimental bandgap of 3.4 eV [18,37], and the shallow donor levels shifted accordingly.

Before considering the defects at the DW, it is worth investigating the formation of defects in bulk FE $PbTiO_3$, within the correction scheme described above [32]. The formation energy of a defect depends on the chemical potentials of the chemical species involved, see Eq. (1). In Fig. (2), we choose to use μ_{O2} and μ_{Pb} as control parameters, and set bounds to these chemical potentials based on thermodynamic considerations (See Supplementary Information). Results corresponding to oxygen-rich $\mu_{O2}=0.00$ eV and μ_{Pb}=-2.98 eV) and oxygen-poor conditions ($\mu_{O2}=-5.50$ eV and μ_{Pb}=0.00 eV) are presented hereafter.

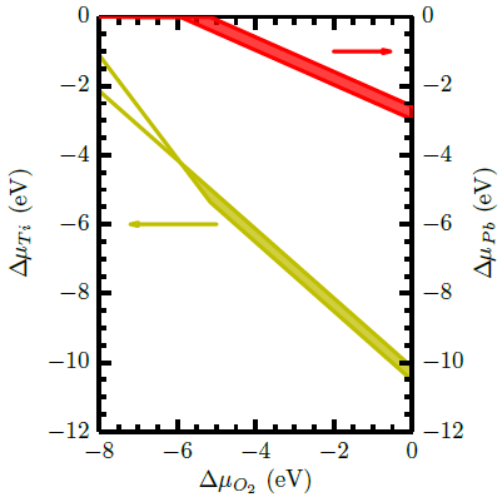

Figure 2. Range of allowed chemical potential for Lead Titanate. In red, $\Delta\mu_{O2}$ and $\Delta\mu_{Pb}$ are the control parameters; In yellow: $\Delta\mu_{O2}$ and $\Delta\mu_{Ti}$ are the control parameters.

2.2. Limitations of the LSDA functional, LSDA+U calculations

In spite of the corrections presented above, the LSDA functional has obvious limitations, that more modern schemes such as hybrid functionals (PBE0, HSE06) are able to overcome. In particular, LSDA is unable to properly describe the possible polaronic localization of holes/electrons released by cationic/anionic vacancies onto the nearby oxygens/titanium. This is due to the self-interaction error (SIE) inherent to the LSDA [38]. Nonetheless, self-trapping of hole polarons is expected to be unfavorable in bulk lead titanate [41], a result that is confirmed in this work (Section 5). Therefore, *in bulk*, the use of hybrid functionals would probably not result in a qualitatively different picture regarding cationic vacancies, although it would certainly improve the quantitative estimates of the various formation energies. Moreover, hybrid functional calculations do not yield a qualitatively different picture regarding oxygen vacancies [22] as discussed here. As a result, the use of the LSDA -- in conjunction with the correction scheme presented above -- to describe defects in lead titanate is a pertinent choice to gain physical insights, and obtain qualitative trends into the formation mechanisms of defects at domain walls in ferroelectrics. It was used in

numerous previous works [15,17,21,33], and provides a substantial gain in computational time with respect to hybrid functionals that include Hartree-Fock exchange.

Here, however, we have complemented, and refined the LSDA description of the cationic vacancies by performing LSDA+U calculations, by applying the U correction onto the p orbitals of the oxygen atoms, as done in a set of recent works [39,41]. This numerical scheme has been shown to provide a correct description of oxygen-type hole polarons in titanates (self-trapping distortions, self-trapping energies, i.e. whether the polaronic state is favored or not over the delocalized state), similar to the one given by hybrid functionals, but with a much lower computational cost [41]. Here this allows us to test the stability of oxygen-type hole polarons, that are expected to be unstable in bulk [41], but could be stabilized at DWs, and to examine whether the holes liberated by Pb/Ti vacancies are delocalized or not.

In order to determine the value of U that minimizes as much as possible the SIE, we performed a set of total energy calculations on a (frozen) polaronic configuration, by varying the charge of the system by fractional values, between 0 and 1. Following Refs. [39,41], that best U parameter is obtained when the variation of energy upon the fractional addition of holes is closest to being linear [41], i.e. it allows to be as close as possible from the piecewise linearity.

From Fig. (3), we find the best U parameter to be 9.5 eV. It is important to note that this value depends on *(i)* the implementation of DFT+U (in the ABINIT code, U is applied inside the PAW spheres), and *(ii)* a given PAW radius for the oxygen atomic dataset, which is here of 1.4 atomic units.

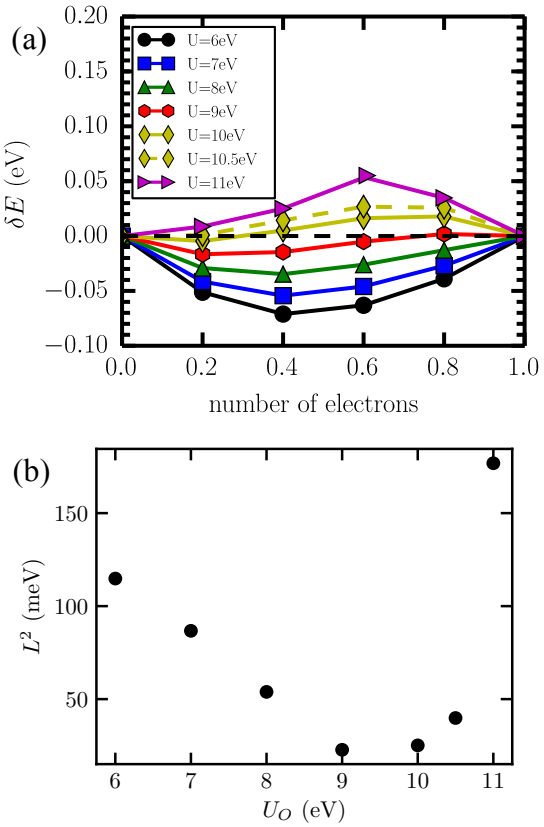

Figure 3. (a) Variation of energy with respect to piecewise linearity with the number of extra electrons in-between *N-1* and *N* electrons, in a (frozen) polaronic configuration. The best *U* parameter must lead to a curve close to the horizontal black dashed line. **(b)** L^2 distance to the behavior of the ideal functional (marked by the horizontal line in panel (a)).

In order to localize holes onto specific oxygens and specific orbitals, we take benefit of the possibility, within the ABINIT code, to control the occupation matrices (OM) of correlated orbitals in DFT+*U*, and mostly apply the following two-step procedure:

(i) first, the system is pre-relaxed with the OMs of the *p* orbitals of the oxygens maintained fixed, with the desired *p* orbital empty, in order to produce the self-trapping distortion associated with the corresponding polaronic configuration;

(ii) then, the constraint on the OMs is relaxed, and the structural optimization restarted from the final configuration obtained at the previous step, with the OMs initialized as in the previous step (and maintained fixed only during a few steps of the first SCF cycle). The system then eventually relaxes to the desired polaronic configuration.

The possibility of having *electronic* polarons is, however, not taken into account by the previous LSDA+*U* scheme (with *U* applied on *p*-oxygen orbitals). The localization of an electron induced by a defect can only be caused in the case of oxygen vacancies. We cannot perform LDA+*U* with a *U* correction on the *d* orbitals of titanium because this destroys the ferroelectric phase in lead titanate, as it prevents the necessary covalency of titanium with a nearby oxygen that causes off-centering of the ions. Nonetheless, localization of electronic charges only occurs in neutral oxygen vacancies or singly ionized oxygen vacancies, which are both too high in energy to occur. According to the work of Shimada *et al.* [22] using the hybrid functional HSE06, neutral oxygen vacancies are more stable than fully ionized vacancies only for Fermi energies that are very high in the gap, and which are forbidden by the negative formation energy of the cationic vacancies. Therefore, oxygen vacancies are mostly fully ionized, and electronic polarons should play a negligible role, if any. Finally, we note that recent works [10] have shown that DWs may be intrinsically ferroelectric, in particular the 180º-DW in PTO, providing here an additional degree of freedom that complexifies the problem. Therefore, for the sake of simplicity, in all our LSDA calculations, the symmetries are maintained, preventing the DW to become intrinsically ferroelectric. However, all the symmetries are suppressed in our LSDA+*U* calculations, allowing for the DW to become intrinsically polar. We show here that the results are not significantly modified, in particular the the defects are still more stable in the DW than in the domain.

3. Results & Discussion

3.1. Vacancies in $PbTiO_3$

3.1.1. Vacancies in bulk

First, we note that in bulk, due to the tetragonal symmetry, the apical oxygen(denoted O_3), is different from those in the plane perpendicular to the *c*-axis (O_1 and O_2). The oxygen vacancy at this apical site is found more stable (by 35 meV for V_O^{+2} similar

to Ref. [21]) than the other two, and we shall only consider this vacancy in the following. As shown in Fig. (4), under any atmosphere, oxygen vacancies are found fully ionized, independently of the value of the Fermi level, in agreement with the work of Yao and Fu [21]. Qualitatively similar results were found with the HSE06 functional, with the doubly charged oxygen vacancy as the most stable for Fermi levels lying 0.4 eV below the conduction band [22]. Note that the existence of intermediate size free electronic polarons and bi-polarons in, for instance WO_3 [42-43] is a clear indication that oxygen vacancies tend to be doubly ionized. However, due to the presence of A-site vacancies (which do not exist in WO_3) in large quantity in lead titanate (see the formation energy of lead compared to oxygen vacancies in oxygen rich conditions for instance in Fig. 4a), it is likely that those electronic polarons are captured and in small quantities in lead titanate. Thus, the fully ionized oxygen vacancy can be associated with empty CB-like electronic states, and should not induce any substantial electronic conductivity in lead titanate.

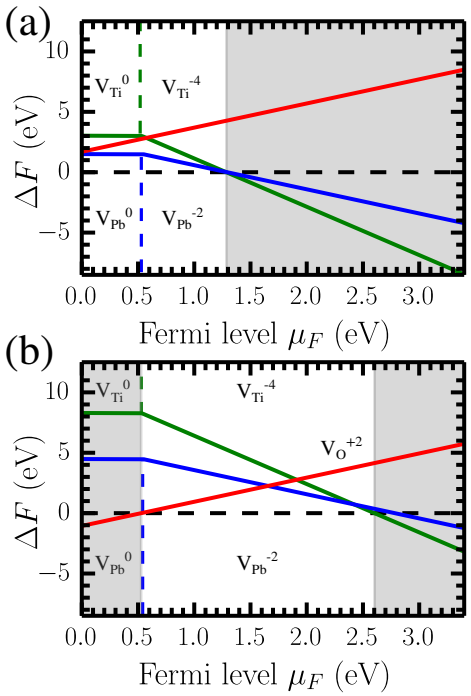

Figure 4. Formation energy of lead, titanium and oxygen vacancies. Only the most stable charge state is represented. The shaded area represents a forbidden range for the Fermi level, due to negative formation energies of the different defects. (a) oxygen-rich atmosphere conditions; (b) oxygen-poor atmosphere conditions. Red, blue and green colors represent oxygen, lead and titanium vacancies.

Cationic vacancies are fully ionized under oxygen-poor conditions (i.e. metal-rich conditions), as shown in Fig. (4.b), and thus barely contribute to conductivity in O-poor conditions. However, in O-rich conditions, a significant portion of cationic vacancies may be in their neutral (or partially ionized) state (although high enough Fermi level should fully ionize the cationic vacancies). In particular, using charge neutrality as in Ref. [44] we found $\mu_F \cong 0.12$ eV in oxygen-rich conditions, and therefore lead vacancies are mostly neutral and charged with one electron, but almost not fully ionized, meaning that holes can be released in the valence band. We will explain, moreover, in the following, that the holes released by the Pb vacancies in the bulk are delocalized and do not form small polarons. These holes contribute therefore to a *p*-type conductivity.

Since oxygen vacancies are still fully ionized, lead titanate is thus expected to be mostly *p*-doped in O-rich conditions. Ionization energies, marked by the changes of slopes and dashed lines in Fig. (4), of both lead and titanium vacancies lie about 0.56 eV above the VBM, and one can therefore tune the *p*-doping of the material by controlling the Fermi level, especially in oxygen rich conditions. Ionization energies of around 0.5-0.6 eV have been deduced from conductivity measurements in $Pb(Zr,Ti)O_3$ thin films [45]. *p*-type conduction is also reported in $Pb(Zr,Ti)O_3$ [46]. These experimental reports agree therefore rather well with our calculations results.

3.1.2. Vacancies at Domain Walls

We now turn to the formation energy of single ion vacancies in a 180° DW. As shown in Fig. (5), we find that each type and charge state of vacancy is always more stable in the DW, as also reported in previous works in a few specific cases [15,17]. Moreover, the stabilization at the DW is much larger for the Ti vacancy than for the Pb and O vacancies: the

difference of formation energy for V_{Ti}^{-4} in the DW is 0.2 eV larger than V_O^{+2}, the latter being itself easier to form compared to V_{Pb}^{-2} by 0.08 eV.

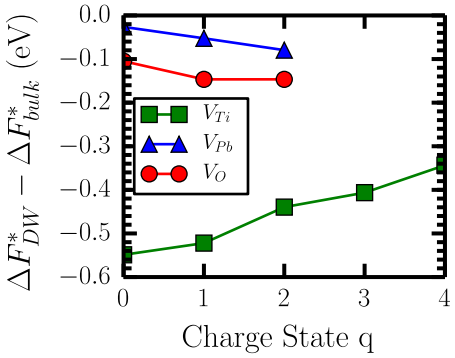

Figure 5. Difference between the formation energy inside the 180°-PbO DW and the bulk region. Among oxygen vacancies, only the apical oxygen is plotted, but the two other types are quantitatively similar. Creating a vacancy inside the DW is always favorable.

Such hierarchy can be understood by looking at the role of each atom species in the appearance of the polarization: it is well-known that the titanium and apical oxygen are crucial to the appearance of the ferroelectric phase [47]. Besides, it was noted by Yao and Fu that creating titanium vacancies was much more detrimental to ferroelectricity in neighboring cells than apical oxygen vacancies [21]. On the opposite, lead vacancies left the polarization almost unaffected. Since the PbO-domain wall is a region of smaller polarization, we expect the aforementioned hierarchy, for creating titanium vacancies in an almost non-polar region (the DW) is more favorable than in a polar region. To shed more light on the preferential formation mechanism of defects at DWs, and since our calculations are run at constant volume to avoid unphysical distortion of the supercell, we looked into the induced stress by a single ion vacancy, as shown in Fig. (6)). We observe that the defect-induced stress is always "more negative/lower"', i.e. has an extra compressive component, when the defect is created in the DW. Difference in strain states between domains and DWs has been recently observed in $TbMnO_3$ [8].

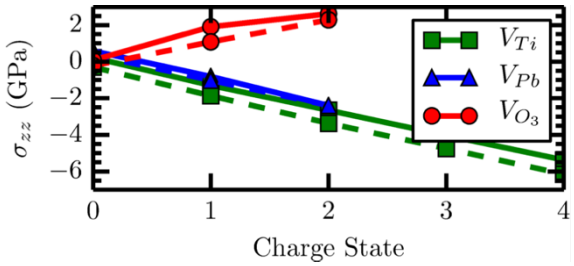

Figure 6. (a) Stress along the polar axis induced by the defect in the bulk (plain lines) and DW region (dashed line). The induced stress is always inferior in the DW : the defect induces an extra compressive (negative) stress compared to the bulk region, consistent with the smaller polarization to kill in the DW.

It is also important to note that the difference between the stress induced in the DW and the stress induced in the bulk exhibits the same hierarchy as the difference between the formation energies: it is always largest for Ti vacancies, is smaller for O vacancies, and almost vanishes for Pb vacancies (Fig. (5) and (6)). The existence of a specific strain field at 180° ferroelectric DWs has recently been revealed [48], and this elastic contribution likely contributes to lower the formation energy of defects in the DW. Defects represent a source to release the intrinsic tensile stress existing in the DW.

4. Discussion

4.1. Phenomenological model

To give further support to this point and explain the hierarchy of defect formation seen in Fig. (5), we interpret the formation energy of defects in a simple phenomenological model. In the bulk region, the energy of a unit cell, with respect to a non-polar and undistorted state, can be expressed as

$$E_{bulk} = \underbrace{-\kappa\eta P^2 + \frac{\alpha}{2}P^2 + \frac{\beta}{4}P^4}_{<0} + c\eta^2 \qquad (2)$$

with P the polarization, and $\eta=(c-c_{cubic})/c_{cubic}$ the strain (P and η along the tetragonal direction) with respect to the cubic *Pm-3m* phase. κ, α and β are the coefficients of this energy expansion, that can be seen as the zero-temperature extension of a Landau-like model, thus $\alpha<0$ here. Approximating the DW as a non-polar region, its energy per unit cell is purely elastic:

$$E_{DW} = c\eta^2 \tag{3}$$

Forming the vacancy of type i in charge state q implies an energy cost related to the breaking of chemical bonds $\Delta E^i_{bond}(q)$ (that we assume equal in the DW and in the bulk). Moreover, the vacancy produces a weakening of the ferroelectric order, that we will model as vanishing of P within $N_{eff}(i,q)$ unit cells around the defect when it is created in a bulk region. Therefore, the energy of the system with one defect, in the bulk as in the DW, can be written (with respect to an undefective non-polar cubic reference) as

$$\begin{aligned} E^i_{bulk}(q) &= \Delta E^i_{bond}(q) + (N_b + N_{DW})c\eta^2 \\ &+(N_b - N_{eff}(i,q))(-\kappa\eta P^2 + \frac{\alpha}{2}P^2 + \frac{\beta}{4}P^4) \end{aligned} \tag{4}$$

$$\begin{aligned} E^i_{DW}(q) &= \Delta E^i_{bond}(q) + (N_b + N_{DW})c\eta^2 \\ &+N_b\left(-\kappa\eta P^2 + \frac{\alpha}{2}P^2 + \frac{\beta}{4}P^4\right) \end{aligned} \tag{5}$$

N_b and N_{DW} being respectively the number of unit cells in the bulk and in the DW part of the supercell. Hence,

$$E^i_{DW}(q) - E^i_{bulk}(q) = \mathrm{N_{eff}}(i,\mathrm{q})\left(-\kappa\eta P^2 + \frac{\alpha}{2}P^2 + \frac{\beta}{4}P^4\right) < 0 \tag{6}$$

$-\kappa\eta P^2 + \alpha P^2/2 + \beta P^4/4$ is the (negative) energy related to the ferroelectric instability (under fixed strain). In the DW, the cost of weakening ferroelectricity has not to be paid, thereby explaining the lower formation energy as well as the ranking of the different vacancies as shown by Fig. (5), considering that $N_{eff}(i,q)$ is obviously highest in the case of the Ti vacancy.

The lattice constant along the tetragonal direction and the atomic positions were varied linearly between the centrosymmetric phase and the tetragonal phase of $PbTiO_3$. The

use of Berry phase calculations of the polarization allowed to fit Eq. (2) and obtain the coefficients $\kappa = 7.986x10^{-3}$ eV.cm^4.μC^{-2}, α=$-2.385x10^{-3}$ eV. cm^4.μC^{-2}, $\beta = 1.142x10^{-8}$ eV.cm^8. μC^{-4} and $C = 4.624x10^3$ eV. It follows from Eq. (6) that the number of effective cells over which the defect destroys the polarization is < 0.5, 0.7, 1.5-2 for Pb, O and Ti vacancies respectively. This confirms the work of Yao and Fu who found the titanium vacancies to be most detrimental to the polarization, while the lead vacancy is termed as being benign to the polarization [21].

In addition, this simple model accounts for the difference in stress when the vacancy is formed in the DW or in the bulk. Remembering that the stress tensor can be expressed as the derivative of the energy with respect to the strain and divided by the volume, we therefore get that the stress induced by a vacancy (i,q) is always more negative in the DW:

$$\Delta\sigma(i,q) = \sigma_{DW}(i,q) - \sigma_{bulk}(i,q) \propto -N_{eff}(i,q)\kappa P^2 \qquad (7)$$

Or said in another way, there is an extra compressive component of the stress tensor when the vacancy is formed in the domain caused by the cost of killing ferroelectricity and its coupling to strain.

4.2. LSDA+U calculations

We now reconsider the previous configurations in the framework of LSDA+U, using U=9.5 eV on the p orbitals of oxygen (see the methods Section for the relevance of the LSDA+U calculations to the present problem, and for the determination of the U value). The symmetry constraints are here fully relaxed. This has two consequences: (i) it allows the DW to become intrinsically ferroelectric, and (ii) hole polarons have the possibility to appear.

First of all, and in agreement with recent works, we find that the DW becomes FE, a polar distortion appearing in the plane of the DW, perpendicular to the polarization in the domains [10]. The atomic displacements are, however, weaker than in bulk as shown in Table

S1 of the Supplementary Information. The DW energy density is 122.9 $mJ.m^{-2}$, very comparable to the energy found previously using the LDA.

Then, we simulate vacancies, and compare their energies when bulk and in the DW. The results are, in most cases, qualitatively similar to the ones obtained within the LSDA. In particular, the Pb vacancy is more stable in the DW independently of its charge state (resp. -0.05, -0.07 and -0.08 eV for V_{Pb}^{0}, V_{Pb}^{-1} and V_{Pb}^{-2}, respectively). In the neutral and partially ionized Pb vacancies, which are respectively double and single acceptors, the holes released do not form polarons. They remain delocalized over the supercell. This result is in good agreement with the one of Shimada *et al.* who studied vacancies in FE PTO using hybrid HSE06 functional and do not observe any polaron formation around the Pb vacancies [22].

The Ti vacancies are also found more stable in the DW than in the domain (-0.69, -0.14, -0.33, -0.30, -0.26 eV from V_{Ti}^{0} to V_{Ti}^{-4}). However, here, we find that hole polarons appear in the case of V_{Ti}^{0} and V_{Ti}^{-1}, i.e. the charge states corresponding to the largest number of released holes. One hole polaron is seen in the case of V_{Ti}^{-1} (bulk case), and three in the case of V_{Ti}^{0} (bulk case), which means that here, among the 4 holes released, one is delocalized and 3 are localized. Once again, this result is in qualitative agreement with the hybrid study of Shimada *et al.*, who observe the presence of 2 polarons associated with V_{Ti}^{0} [22].

Finally, all charge states of the oxygen vacancy are found to be most stable in the domain wall, with formation energies lowered by 0.07, 0.14 and 0.14 eV compared to the bulk, for V_{O}^{0}, V_{O}^{+1} and V_{O}^{+2} respectively. Those results confirm *(i)* what had been seen with the bare LDA functional, that is that point defects are always more stable in the domain wall and *(ii)* that the intrinsic FE of the DW does not deeply modify these results.

4.3. Free Holes in $PbTiO_3$

We have seen that cationic vacancies liberate holes, that may, under the effect of thermal agitation, move and diffuse in the bulk. We now examine their behavior as free entities, i.e. far from defects. One question is whether they are delocalized, or localized on an oxygen atom under the form of a self-trapped hole (STH) polaron. The following calculations thus use the LSDA+U, with $U=9.5$ eV on the p states of oxygen.

4.3.1. Self-trapped hole polarons versus delocalized holes in bulk

Using the two-step procedure described in the Methods Section, we first simulate the self-trapped hole polaron in bulk tetragonal FE PTO (here we use a FE 120-atom unit cell without DW). The hole may be localized on an apical oxygen (O_3), or on an equatorial oxygen ($O_{1/2}$). In the latter case, the hole may occupy an orbital parallel to the FE distortion, or perpendicular to it. The three cases have been examined, and are shown in Fig. 7. We note these three entities, respectively, $O_{O3}^{\bullet}$, $O_{O1/2,//}^{\bullet}$, and $O_{O1/2,\perp}^{\bullet}$. We also calculate the delocalized hole. We find that the most stable site for the polaron is $O_{O1/2,\perp}^{\bullet}$.

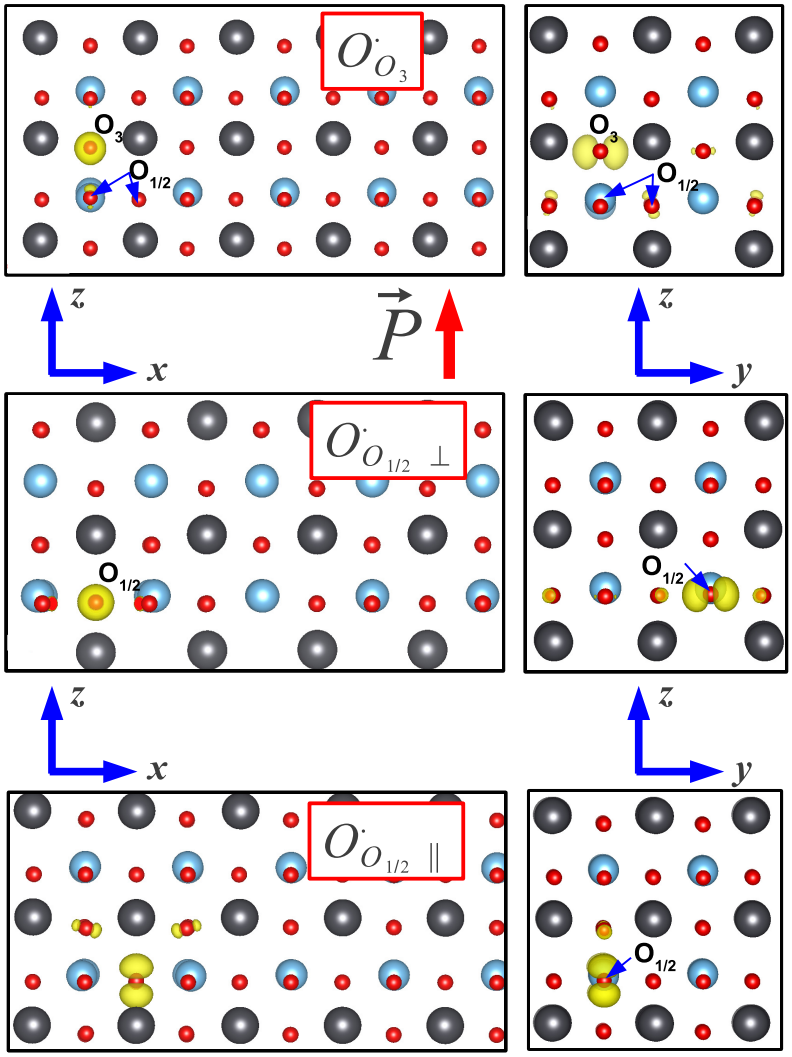

Figure 7. Isosurfaces of the hole state in the case of a self-trapped hole polaron in bulk tetragonal $PbTiO_3$, in the three possible configurations.

However, the hole polaron is found less stable than the delocalized hole in all three cases, by respectively 150, 194 and 126 meV, showing that *holes in bulk PTO are not fully localized*. Therefore, our results in ferroelectric PTO state confirm and complete the work of Erhart *et al.*, who found the hole polaron in paraelectric PTO less stable than the delocalized hole by 0.24 eV [41].

4.3.2. *Self-trapped hole polarons versus delocalized holes at Domain Walls*

Next, we simulate the hole polaron as trapped on an oxygen in the DW. Two configurations are possible, whether the empty *2p* orbital is parallel or perpendicular to the polarization in the domains. An isosurface of the hole state in the optimized atomic configurations is drawn on Fig. 8 in both cases. In the DW, we calculate the self-trapping energy of holes to be between 85 and 8 meV, that is, self-trapped hole (STH) polarons are still disfavored compared to band holes, although the self-trapping energy is largely reduced with respect to the values found in bulk. Interestingly, a recent experiment has evidenced specific polaronic relaxation at 180˚ domain walls in the dielectric response of single crystal lithium niobate samples [49]. The large reduction of the self-trapping energy at the domain wall found in the present work is consistent with their findings that polarons may be trapped in the domain wall.

It is noteworthy that the hole orbital is impacted by the ferroelectric distortion: when the empty *2p* orbital is parallel to the polarization, it appears as slightly bent (Fig. (8.a)), and hybridized with *2p* orbitals corresponding to the two oxygens that are made closer by the FE distortion, which are in opposite directions in the two domains. Such hybridization could further help stabilizing STH at locally charged domain wall kinks, which have recently been observed [50].

STH polarons are therefore unlikely in FE $PbTiO_3$, except in DWs where they could appear almost as stable as band holes.

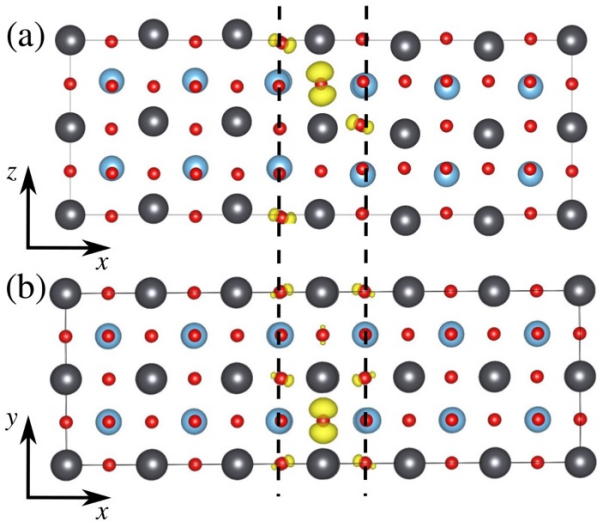

Figure 8. Isosurfaces of the hole state in the case of a self-trapped hole polaron localized in the domain wall. (a) The empty *2p* orbital is parallel to the FE distortion; (b) The empty *2p* orbital is perpendicular to the FE distortion.

5. Conclusion

In this work, we have performed density-functional calculations to understand how single ion vacancies behave, in bulk and at the 180° PbO-DW of $PbTiO_3$. All the vacancies, in all possible charge states, are more stable in the DW than in the bulk, the higher stabilization occurring in the case of the Ti vacancy. Based on a simple phenomenological model, we explain that the ions carrying the most polarization are the ones for which the energy difference between the bulk and DW formation energy is the greatest. This model could be general to other ferroic order parameters, and thus predicts that defects affecting critically the ferroic order parameter will be way easier to form in a domain wall. This is however counterbalanced by the natural tendency of such defects to have a high cost of formation in the domain, precisely as they tend to destroy the ferroic phase. Oxygen vacancies are found fully ionized independently of the thermodynamic conditions, thus liberating no electron, while cationic vacancies may be neutral or partially ionized in strongly oxidizing conditions, the most common ones being V_{Pb}^{0} and V_{Pb}^{-1}. The holes liberated by these two kinds of acceptor defects are mainly delocalized and could be self-trapped in DWs.

Acknowledgements

We acknowledge National Computing Center for Higher Education (CINES) for granting access to its computing facility (project c2015097227), CNRS and CEA agencies. C.P. and B.D. thank a public grant overseen by the French National Research Agency (ANR) as part of the "Investissements d'Avenir" program (reference: ANR-10-LABX-0035, Labex NanoSaclay). L.B. thanks the Department of Energy, Office of Basic Energy Sciences, under contract ER-46612.

References

[1] J. Seidel, L. W. Martin, Q. He, Q. Zhan, Y.-H. Chu, A. Rother, M. E. Hawkridge, P. Maksymovych, P. Yu, M. Gajek, N. Balke, S. V. Kalinin, S. Gemming, F. Wang, G. Catalan, J. F. Scott, N. Spaldin, J. Orenstein, R. Ramesh, *Nat. Mater.* **8**, 229 (2009).

[2] S. Farokhipoor and B. Noheda, *Phys. Rev. Lett.* **107**, 127601 (2011).

[3] P. Maksymovych, J. Seidel, Y. H. Chu, P. Wu, A. P. Baddorf, L.-Q. Chen, S. V. Kalinin, R. Ramesh, *Nano Letters* **11**, 1906 (2011).

[4] J. Guyonnet, I. Gaponenko, S. Gariglio, P. Paruch, *Adv. Mater.* **23**, 5377 (2011).

[5] A. Aird, E. K. H. Salje, *J. Phys.: Condens. Matt.* **10**, L377 (1999).

[6] S. Van Aert, S. Turner, R. Delville, D. Schryvers, G. Van Tendeloo, E. K. H. Salje, *Adv. Mater.* **24**, 523 (2012).

[7] J. F. Scott, E. K. H. Salje, M. A. Carpenter, *Phys. Rev. Lett.* **109**, 187601 (2012).

[8] S. Farokhipoor, C. Magén, S. Venkatesan, J. Íñiguez, C. J. M. Daumont, D. Rubi, E. Snoeck, M. Mostovoy, C. de Graaf, A. Müller, M. Döblinger, C. Scheu, B. Noheda, *Nature* **515**, 379 (2014).

[9] E. K. H. Salje, O. Aktas, M. A. Carpenter, V. V. Laguta, J. F. Scott, *Phys. Rev. Lett.* **111**, 247603 (2013).

[10] J. C. Wojdel and J. Íñiguez, *Phys. Rev. Lett.* **112**, 247603 (2014).

[11] G. Catalan, J. Seidel, R. Ramesh, J. F. Scott, *Rev. Mod. Phys.* **84**, 119 (2012).

[12] J. Seidel, G. Singh-Bhalla, Q. He, S. Y. Yang, Y.-H. Chu, R. Ramesh, *Phase Trans.* **86**, 53 (2013).

[13] L. J. McGilly, P. Yudin, L. Feigl, A. K. Tagantsev, N. Setter, *Nat. Nanotech.* **10**, 145 (2015).

[14] J. Whyte, M. Gregg, *Nat. Comm.* **6**, 7361 (2015).

[15] L. He, D. Vanderbilt, *Phys. Rev. B* **68**, 134103 (2003).

[16] M. Calleja, M. Dove, E. K. H. Salje, *J. Phys.: Condens. Matt.* **15**, 2301 (2003).

[17] A. Chandrasekaran, D. Damjanovic, N. Setter, N. Marzari, *Phys. Rev. B* **88**, 241116 (2013).

[18] J. F. Scott, *Ferroelectric Memories*, Springer Science & Business Media (2000).

[19] V. C. Lo, *J. Appl. Phys.* **92**, 6778 (2007).

[20] P. Erhart, R.-A. Eichel, P. Träskelin, K. Albe, *Phys. Rev. B* **76**, 174116 (2007).

[21] Y. Yao, H. Fu, *Phys. Rev. B* **84**, 064112 (2011).

[22] T. Shimada, T. Ueda, J. Wang, T. Kitamura, *Phys. Rev. B* **87**, 174111 (2013).

[23] D. Emin, *Polarons*, Cambridge University Press, Cambridge (2012).

[24] X. Gonze, B. Amadon, P. M. Anglade, J. M. Beuken, F. Bottin, P. Boulanger, F. Bruneval, D. Caliste, R. Cara- cas, M. Côté, T. Deutsch, L. Genovese, P. Ghosez, M. Giantomassi, S. Goedecker, D. R. Hamann, P. Hermet, F. Jollet, G. Jomard, S. Leroux, M. Mancini, S. Mazevet, M. J. T. Oliveira, G. Onida, Y. Pouillon, T. Rangel, G. M. Rignanese, D. Sangalli, R. Shaltaf, M. Torrent, M. J. Verstraete, G. Zerah and J. W. Zwanziger, *Comp. Phys. Comm.* **180**, 2582 (2009).

[25] W. Kohn, L. Sham, *Phys. Rev.* **140**, A1133 (1065).

[26] J. P. Perdew, Y. Wang, *Phys. Rev. B* **45**, 13244 (1992).

[27] P. E. Blöchl, Phys. Rev. B **50**, 17953 (1994).

[28] M. Torrent, F. Jollet, F. Bottin, G. Zérah, X. Gonze, *Comp. Mater. Sci.* **42**, 337 (2008).

[29] B. Meyer, D. Vanderbilt, *Phys. Rev. B* **65**, 104111 (2002).

[30] G. Sághi-Szabó, R. Cohen, H. Krakauer, *Phys. Rev. Lett.* **80**, 4321 (1998).

[31] F. Jona, G. Shirane, *Ferroelectric Crystals*, Pergamon Press, Oxford (1962).

[32] S. Lany, A. Zunger, *Phys. Rev. B* **78**, 235104 (2008).

[33] Z. Alahmed, H. Fu, *Phys. Rev. B* **76**, 225101 (2007).

[34] C. Persson, Y. J. Zhao, S. Lany, A. Zunger, *Phys. Rev. B* **72**, 035211 (2005).

[35] G. Makov, M. Payne, *Phys. Rev. B* **51**, 4014 (1995).

[36] J. Lento, Mozos, R. M. Nieminen, *J. Phys.: Condens. Matt.* **14**, 2637 (2002).

[37] R. Schafranek, S. Li, F. Chen, W. Wu, A. Klein, *Phys. Rev. B* **84**, 045317 (2011).

[38] J. P. Perdew, R. G. Parr, M. Levy, J. L. Balduz, *Phys. Rev. Lett.* **49**, 1961 (1982).

[39] A. Lindman, P. Erhart, G. Wahnström, *Phys. Rev. B* **94**, 075204 (2016).

[40] J. Dionot, G. Geneste, C. Mathieu, N. Barrett, *Phys. Rev. B* **90**, 014107 (2014).

[41] P. Erhart, A. Klein, D. Åberg, B. Sadigh, *Phys. Rev. B* **90**, 035204 (2014).

[42] O. F. Schirmer, E. Salje, *Sol. State Comm.* **33**, 333 (1980).

[43] O. F. Schirmer, E. Salje, *J. Phys. C: Solid St. Phys.* **13**, L1067 (1980).

[44] T. R. Paudel, S. S. Jaswal, E. Y. Tsymbal, *Phys. Rev. B* **85**, 104409 (2012).

[45] B. Nagaraj, S. Aggarwal, T. K. Song, T. Sawhney, R. Ramesh, *Phys. Rev. B* **59**, 16022 (2007**)**.

[46] B. A. Boukamp, M. T. N. Pham, D. H. A. Blank, H. J. M. Bouwmeester, *Sol. State Ion.* **170**, 239 (2004).

[47] R. E. Cohen, *Nature* **358**, 136 (1992).

[48] K. Shapovalov, P. Yudin, A. K. Tagantsev, E. A. Eliseev, A. N. Morozovska, N. Setter, *Phys. Rev. Lett.* **113**, 207601 (2014).

[49] G. F. Nataf, O. Aktas, T. Granzow, E. K. H. Salje, *J. Phys.: Condens. Matter* **28**, 015901 (2016).

[50] J. Gonnissen, D. Batuk, G. F. Nataf, L. Jones, A. M. Abakumov, S. Van Aert, D. Schryvers, E. K. H Salje, *Adv. Func. Mater.* **26**, 7599 (2017).